

# Stress analysis for long thermoelastic rods with mixed boundary conditions

A. O. El-Refaie · A. Y. Al-Ali · K. H. Almutairi ·  
E. K. Rawy

Received: 31 January 2016 / Accepted: 16 December 2016 / Published online: 28 March 2017  
© Springer Science+Business Media Dordrecht 2017

**Abstract** A hybrid method involving boundary analysis and boundary collocation is used to obtain an approximate solution for a plane problem of uncoupled thermoelasticity with mixed thermal and mechanical boundary conditions in a square domain with one curved side. The unknown functions in the cross-section are obtained in the form of series expansions in Cartesian harmonics. A boundary analysis reveals the singular behavior of the solution at the transition points. In order to simulate the weak discontinuities of the temperature function and the discontinuities of stress, these expansions are enriched with proper harmonic functions with a singular behavior at the transition points. The results are discussed, and the functions of practical interest are represented on the boundary and also inside the domain. The locations where possible debonding of the fixed part of the boundary may take place are noted.

**Keywords** Boundary integral method · Cartesian harmonics · Mixed boundary conditions · Plane uncoupled thermoelasticity · Singular behavior

**Mathematics Subject Classification** 74B05 · 74G70 · 65L60

## 1 Introduction

The aim of thermoelastostatics is to evaluate temperature, deformation, and stress in structures under various thermal and mechanical loads. Several monographs have been devoted to the subject [1–3]. Different mathematical tools, both analytical and numerical, have been used to tackle problems of thermoelasticity. Shanker and Dhaliwal [4] use integral representations to study asymmetric thermoelasticity. Singh and Dhaliwal [5] consider mixed boundary-value problems of thermoelastostatics and electrostatics by Fourier transform and subsequent reduction to integral equations. Abou-Dina and Ghaleb [6] present a boundary integral method for the solution of plane strain problems of uncoupled thermoelasticity in stresses using real functions in simply connected cross-sections under homogeneous boundary conditions. Computational aspects are considered in [7], with reference to the ellipse [8]. An approach by complex analysis may be found in [9]. Han and Hasebe [10] derive Green's function for the infinite plane with a hole under adiabatic or isothermal conditions. Şeremet, and Şeremet and Bonnet [11–18] present integral

A. O. El-Refaie · A. Y. Al-Ali · K. H. Almutairi · E. K. Rawy (✉)  
Department of Mathematics, Faculty of Science, Cairo University, 12613 Giza, Egypt  
e-mail: enaamkhalifa@yahoo.com

representations for thermoelastic Green's functions for Poisson's equation with examples for various geometries of the cross-section. Meleshko [19–21] evaluates thermal stresses in an isotropic rectangular plate or a long bar with rectangular cross-section by the superposition method using a Fourier series with examples. Thermoelastic interaction with electromagnetic fields may be found in [22,23].

The potential theory is a main component of thermoelastostatics for homogeneous, isotropic media. Applications of this theory are found in [24–26]. Solutions to many problems of thermostatics and elastostatics are found in the literature. The method of fundamental solutions was presented by Fairweather and Karageorgis ([27] and references therein). The adaptivity of the method when applied to problems with boundary singularities was pointed out through incorporation into the solution of proper local expansions. Abou-Dina [28] treats some harmonic and biharmonic problems by Trefftz's method. Abou-Dina and Ghaleb [29] present approximate solutions to some regular and singular harmonic boundary-value problems in rectangular regions by a boundary Fourier expansion. Read [30] uses analytic series to solve harmonic problems with mixed boundary conditions. Similar problems are treated in [31,32]. Finite Fourier transform is used by El-Dhaba et al. [33] to investigate the deformation of a rectangle. The same method is used by El-Dhaba and Abou-Dina [34] to study the thermal stresses arising in a long bar with rectangular cross-section due to a variable heat source.

Numerical techniques and semi-analytic methods are necessary tools when the shape of the boundary, or the type of boundary conditions, is complicated. Boundary integral formulations are popular as they rely on the well-developed theory of Fredholm integral equations and for less computational effort. Integral equation methods in potential theory and in elastostatics are presented in [24,25]. Altiero and Gavazza [35] propose a unified boundary integral method for linear elastostatics. Heise [36,37] applies boundary integral equations to treat problems of elastostatics with discontinuous boundary conditions. Koizumia et al. [38] present a boundary integral equation analysis for thermoelastostatics using thermoelastic potential. Constanda [39,40] applies a boundary integral formulation to solve the Dirichlet and Neumann problems of elasticity. Different applications of integral equation methods are presented in [41–43]. A modified Sinc-collocation method for two-dimensional elliptic boundary-value problems is treated in [44]. Elliotis et al. [45] present a boundary integral method adapted to the biharmonic equation with crack singularities. Li et al. [46] present a numerical solution for models of linear elastostatics involving crack singularities. A review of boundary integral methods in the theory of elasticity of hemitropic materials may be found in [47]. Cheng et al. [48] investigated mechanical quadrature methods and extrapolation algorithms for boundary integral equations with linear boundary conditions in elasticity. Meshless methods are investigated in [49–51].

Mixed boundary conditions are treated in [5]. Helsing [52] proposed an integral equation method to solve Laplace's equation under mixed Dirichlet and Neumann conditions on contiguous parts of the boundary, and the problem of elastostatics under mixed conditions. Boundary-value problems of mixed type with applications are considered by Khuri [53]. Gjam et al. [54] give an approximate solution to the problem of an ellipse with half boundary fixed and the other half under given pressure, and they use expansions involving a harmonic function with logarithmic singular behavior at the boundary.

Corner boundary points lead to singular behavior of the solution. This influences the efficiency of computations. An extensive treatment of singularities exists in the literature for the Laplacian, as well as for elastic problems. Williams [55] discusses stress singularities in plates. An algorithm for plane potential solving problems with mixed boundary conditions involving extraction of singularities is treated in [56]. Gusenkova and Pleshchinskii [57] construct complex potentials with logarithmic singularities for elastic bodies with a defect along a smooth arc. Abou-Dina and Ghaleb [29] introduce logarithmic singularities on the boundary of rectangular domains for approximate solutions to Laplacian boundary-value problems with mixed boundary conditions. Kotousov and Lew [58] study stress singularities under various boundary conditions at angular corners of plates. El-Seadawy et al. [59] used boundary integrals to solve 2D problems with mixed geometry, including parts of an ellipse or a circle. The corners are smoothed locally by polynomial functions. Helsing and Ojala [60] treated corner singularities for elliptic problems by boundary integral equation methods on domains with a large number of corners and branching points. Helsing [61] presented a fast and stable algorithm for treating singular integral equations on piecewise smooth curves. Mixed-type boundary conditions at corners were treated in [29,46,62,63]. Gillman et al. [64] presented simplified techniques for discretizing the boundary integral equations in 2-D domains with corners. Local mesh

refinement is used, instead of the classical technique relying on the expansion of the unknowns near the corner by special basis functions that simulate the singularity.

In the present paper, the problem of uncoupled thermoelasticity is solved in a square domain with one curved side. The heat problem has three types of boundary condition on different parts of the boundary and a transition point at a corner. The mechanical boundary conditions are of mixed type: there is a variable pressure on half of the boundary, and the other half is fixed. A semi-analytical scheme presented in [54] for the purely elastic problem is applied here: The problem is replaced with two subproblems of uncoupled thermoelasticity with a common solution. The mechanical conditions for these two subproblems are different: One subproblem is the first fundamental problem of elasticity, i.e., with given stresses on the boundary, while the other subproblem is the second fundamental problem of elasticity, i.e., with given displacements on the boundary. Each of these two subproblems has the prescribed entries on part of the boundary, while the other part carries unknown values to be determined as part of the solution. These two subproblems yield a system of boundary integral equations following the framework proposed in [7]. A simple discretization procedure finally reduces the system of integral equations to a rectangular system of linear algebraic equations which is solved by Least Squares. The obtained results on the boundary clearly show a singular behavior of the stress components at the two transition boundary points as expected. For the solution inside the domain, proper expansions of the two basic harmonic functions are proposed in terms of Cartesian harmonics. To take into account the singularities, the stress function is enriched with a harmonic function with weak singularities (in the second derivatives) at the two separation points. After truncation of the expansions, the coefficients are determined by the boundary collocation method using the previously obtained values of the unknown functions on the boundary. Two-dimensional boundary plots and three-dimensional plots in the domain of the normal cross section are provided for the functions of practical interest. The results and the efficiency of the used scheme are discussed. All figures were produced using Mathematica 9.0 software.

The problem under consideration models a long elastic pad support and thereby is of practical importance. The stresses applied on one part of the boundary represent the influence of the body resting on the foundation. The chosen form of the boundary deviates from being regular and, moreover, involves corner points and mixed boundary conditions. These factors are challenging from the computational point of view and clearly indicate the efficiency of the proposed method. The boundary shape, as well as the chosen boundary functions, are only representative. Other settings may be considered as well, for example, adding a shear stress on the boundary or treating a multilayer foundation [65]. The shape of the singular function, however, will differ from one case to the other.

## 2 Problem description

The uncoupled plane theory of thermoelasticity is used to solve the problem of deformation of a long cylinder made from an isotropic, homogeneous, elastic material under mixed thermal and mechanical boundary conditions by a boundary integral method. The normal cross-section  $D$  of the cylinder is simply connected and bounded by a contour  $C$  in the form of a square with one curved side as shown in Fig. 1, where the boundary conditions for temperature, tension, and displacements are represented.

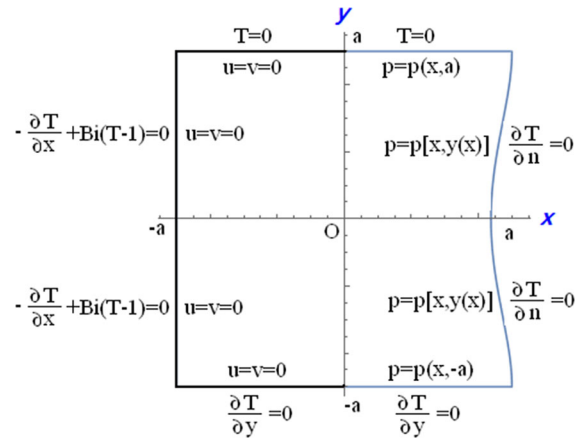
The governing equations, boundary conditions and other closure relations are formulated in an orthogonal system of Cartesian coordinates  $(x, y)$  with origin  $O$  inside the domain  $D$ . The lateral surface of the cylinder is partly acted upon by forces in the plane of the cross-section, while the remaining part is fixed. Heat exchange with the ambient medium takes place through one part of the boundary. The other parts are either kept at fixed temperature or thermally isolated. No body forces or heat sources are considered.

The contour  $C$  is represented by the parametric equations:

$$x = x(\theta), \quad y = y(\theta), \tag{1}$$

where  $\theta$  is the usual polar angle.

**Fig. 1** Problem formulation



The vectors  $\boldsymbol{\tau}$  and  $\boldsymbol{n}$  denote the unit vector tangent to  $C$  at any arbitrary point on the contour and the unit outwards normal at this point, respectively. These two vectors form a basis that is similar to the basis of the orthogonal Cartesian system of coordinates. One has:

$$\boldsymbol{\tau} = \frac{\dot{x}}{\omega} \mathbf{i} + \frac{\dot{y}}{\omega} \mathbf{j} \quad \text{and} \quad \boldsymbol{n} = \frac{\dot{y}}{\omega} \mathbf{i} - \frac{\dot{x}}{\omega} \mathbf{j}, \tag{2}$$

the dot denotes differentiation with respect to the parameter  $\theta$ , i.e., along the tangent, and

$$\omega = \sqrt{\dot{x}^2 + \dot{y}^2}. \tag{3}$$

### 3 Basic equations

The governing equations are listed below without proof, in accordance with [6, 7]. The exact solution for temperature is given in closed form for the square domain (cf. in [66]). It has been analyzed in [29]. This analysis will be used here to accommodate the weak singular behavior of temperature at one vertex.

#### 3.1 Equation of thermostatics

$$\nabla^2 T = 0, \tag{4}$$

where  $T$  is measured from a reference temperature  $T_0$ .

#### 3.2 Equations of equilibrium

In the approach by stresses, the identically non-vanishing components of stress in the cross section plane are derived from a stress function  $U$  by

$$\sigma_{xx} = \frac{\partial^2 U}{\partial y^2}, \quad \sigma_{xy} = -\frac{\partial^2 U}{\partial x \partial y}, \quad \sigma_{yy} = \frac{\partial^2 U}{\partial x^2}, \tag{5}$$

and this function satisfies the biharmonic equation in virtue of the compatibility condition:

$$\nabla^4 U = 0. \tag{6}$$

The generalized Hooke’s law reads:

$$\begin{aligned} \sigma_{xx} &= \frac{\nu E}{(1 + \nu)(1 - 2\nu)} \left( \frac{\partial u}{\partial x} + \frac{\partial v}{\partial y} \right) + \frac{E}{(1 + \nu)} \frac{\partial u}{\partial x} - \frac{\alpha E}{(1 - 2\nu)} T, \\ \sigma_{xy} &= \frac{E}{2(1 + \nu)} \left( \frac{\partial u}{\partial y} + \frac{\partial v}{\partial x} \right), \\ \sigma_{yy} &= \frac{\nu E}{(1 + \nu)(1 - 2\nu)} \left( \frac{\partial u}{\partial x} + \frac{\partial v}{\partial y} \right) + \frac{E}{(1 + \nu)} \frac{\partial v}{\partial y} - \frac{\alpha E}{(1 - 2\nu)} T, \end{aligned} \tag{7}$$

where  $E$ ,  $\nu$  and  $\alpha$  denote Young’s modulus, Poisson’s ratio, and the coefficient of linear thermal expansion, respectively, and  $u$ ,  $v$  denote the displacement components.

The stress function  $U$  solving the Eq. (6) is represented through two harmonic functions as

$$U = x \phi + y \phi^c + \psi, \tag{8}$$

where the superscript “ $c$ ” denotes the harmonic conjugate.

The stress components are expressed in terms of  $\phi$  and  $\psi$  as

$$\begin{aligned} \sigma_{xx} &= x \frac{\partial^2 \phi}{\partial y^2} + 2 \frac{\partial \phi^c}{\partial y} + y \frac{\partial^2 \phi^c}{\partial y^2} + \frac{\partial^2 \psi}{\partial y^2}, \\ \sigma_{xy} &= -x \frac{\partial^2 \phi}{\partial x \partial y} - y \frac{\partial^2 \phi^c}{\partial x \partial y} - \frac{\partial^2 \psi}{\partial x \partial y}, \\ \sigma_{yy} &= x \frac{\partial^2 \phi}{\partial x^2} + 2 \frac{\partial \phi}{\partial x} + y \frac{\partial^2 \phi^c}{\partial x^2} + \frac{\partial^2 \psi}{\partial x^2}. \end{aligned} \tag{9}$$

The following representation of the Cartesian displacement components  $u$  and  $v$  may be easily obtained:

$$\begin{aligned} \frac{E}{(1 + \nu)} u &= -\frac{\partial U}{\partial x} + 4(1 - \nu) \phi + \frac{E}{1 + \nu} u_T, \\ \frac{E}{(1 + \nu)} v &= -\frac{\partial U}{\partial y} + 4(1 - \nu) \phi^c + \frac{E}{1 + \nu} v_T, \end{aligned}$$

where

$$u_T = \alpha(1 + \nu) \int_{M_0}^M (T \, dx - T^c \, dy) \quad \text{and} \quad v_T = \alpha(1 + \nu) \int_{M_0}^M (T^c \, dx + T \, dy). \tag{10}$$

are the temperature displacements. The integrals in (10) are noted in complex form in ([1], p. 323). Point  $M \in D$  is the general point where the displacements are calculated, while the initial point  $M_0$  is adequately chosen in the cross-sectional domain or on the boundary  $C$ . Rewritten in terms of  $\phi$  and  $\psi$ , relations (10) yield:

$$\begin{aligned}
 2\mu u &= (3 - 4\nu)\phi - x \frac{\partial \phi}{\partial x} - y \frac{\partial \phi^c}{\partial x} - \frac{\partial \psi}{\partial x} + 2\mu u_T, \\
 2\mu v &= (3 - 4\nu)\phi^c - x \frac{\partial \phi}{\partial y} - y \frac{\partial \phi^c}{\partial y} - \frac{\partial \psi}{\partial y} + 2\mu v_T,
 \end{aligned}
 \tag{11}$$

where  $\mu = E/2(1 + \nu)$  is the modulus of rigidity of the elastic material.

It is thus clear that in the absence of heat sources the only contribution of temperature to the elastic solution is confined to the additional displacements  $u_T$  and  $v_T$  in the expressions for the displacement.

#### 4 Accompanying conditions

It is well-known that the solution of strain problems in stresses involves some arbitrariness (cf. [67]). For any numerical or semi-analytical approach to the problem such an arbitrariness must be completely eliminated. In order to obtain a unique solution to the considered problem, the basic field equations and boundary conditions are complemented by conditions for removal of rigid body motion, and by other conditions which have no physical insight. Details may be found in the above-mentioned reference.

##### 4.1 Boundary conditions

The considered problem involves mixed thermal and mechanical boundary conditions.

- *Dirichlet thermal condition*

$T(\theta) = h(\theta)$ , where  $h$  is a given function on the boundary.

- *Neumann thermal condition*

$\frac{\partial T}{\partial n} = g(\theta)$ , where  $g$  is a given function on the boundary.

- *Robin thermal condition*

$\frac{\partial T}{\partial n} + Bi [T(\theta) - T_e(\theta)] = 0$ ,

where  $Bi$  is Biot constant and  $T_e$  the external (ambient) temperature.

- *The first fundamental problem of elasticity*

Assuming that the density of the given distribution of the total external surface forces is:

$$\mathbf{f} = f_x \mathbf{i} + f_y \mathbf{j} = \sigma_{nx} \mathbf{i} + \sigma_{ny} \mathbf{j},$$

the boundary conditions take the form:

$$\begin{aligned}
 f_x &= (x\phi_{yy} + 2\phi_y^c + y\phi_{yy}^c + \psi_{yy}) \frac{\dot{y}}{\omega} + (x\phi_{xy} + y\phi_{xy}^c + \psi_{xy}) \frac{\dot{x}}{\omega}, \\
 f_y &= -(x\phi_{xy} + y\phi_{xy}^c + \psi_{xy}) \frac{\dot{y}}{\omega} - (x\phi_{xx} + 2\phi_x^c + y\phi_{xx}^c + \psi_{xx}) \frac{\dot{x}}{\omega}.
 \end{aligned}
 \tag{12}$$

- *The second fundamental problem of elasticity*

Assuming that the displacement vector is

$$\mathbf{d} = d_x \mathbf{i} + d_y \mathbf{j} = d_n \mathbf{n} + d_\tau \boldsymbol{\tau},$$

the boundary conditions take the form:

$$\begin{aligned}
 2\mu d_x &= (3 - 4\nu)\phi - x\phi_x - y\phi_x^c - \psi_x + 2\mu u_T, \\
 2\mu d_y &= (3 - 4\nu)\phi^c - x\phi_y - y\phi_y^c - \psi_y + 2\mu v_T.
 \end{aligned}$$

### 4.2 Elimination of rigid body motion

The boundary conditions used in the problem under consideration prohibit any rigid body motion in the elastic solution.

In setting any of the above accompanying conditions, one needs the first and the second derivatives of any harmonic function  $f$  with respect to  $x$  and  $y$  on the boundary. These may be calculated as in Appendix 2.

### 4.3 Additional simplifying conditions

The following supplementary purely mathematical conditions are adopted for simplicity at the point of the boundary where  $\theta = 0$ :

$$\begin{aligned} x(0)\phi(0) + y(0)\phi^c(0) + \psi(0) &= 0, \\ x(0)\phi^c(0) - y(0)\phi(0) + \psi^c(0) &= 0, \\ x(0)\phi_x(0) + \phi(0) + y(0)\phi_x^c(0) + \psi_x(0) &= 0, \\ x(0)\phi_y(0) + \phi^c(0) + y(0)\phi_y^c(0) + \psi_y(0) &= 0, \\ T^c(0, 0) &= 0. \end{aligned}$$

All the above mentioned mechanical equations and conditions can be transformed into boundary integral equations by using the boundary integral representation of the basic harmonic functions  $\phi$  and  $\psi$  (and their conjugates) together with the Cauchy–Riemann relations. For details, the reader is referred to [6,7]. This approach allows one to find the values of all the unknown functions on the boundary. Because of the discontinuities occurring at the transition points, the results are expected to involve some error. Our aim at this stage is to use such boundary analysis to put in evidence the singular behavior of the solution and to make a guess about the types of singularity occurring at the transition points of the thermal and mechanical boundary conditions.

## 5 Calculation of the harmonic functions inside the domain

For the case under consideration, the analytical formulas allowing one to calculate the unknown functions inside the cross-sectional domain are taken as expansions in terms of Cartesian harmonics, with coefficients to be determined by the boundary collocation method after truncation. These expansions are enriched with properly chosen harmonic functions having singular behaviors at the transition points of the thermal and mechanical boundary conditions:

$$\begin{aligned} T = D + r_0x + s_0y + t_0xy + w_0(x^2 - y^2) + \sum_{n=1}^{\infty} r_n \cos nx \cosh ny + \sum_{n=1}^{\infty} s_n \cos nx \sinh ny \\ + \sum_{n=1}^{\infty} t_n \sin nx \cosh ny + \sum_{n=1}^{\infty} w_n \sin nx \sinh ny + q_1\eta(x, y) + q_2\gamma(x, y), \end{aligned}$$

$$\begin{aligned} T^c = F - s_0x + r_0y + 2w_0xy - \frac{1}{2}t_0(x^2 - y^2) + \sum_{n=1}^{\infty} w_n \cos nx \cosh ny + \sum_{n=1}^{\infty} t_n \cos nx \sinh ny \\ - \sum_{n=1}^{\infty} s_n \sin nx \cosh ny - \sum_{n=1}^{\infty} r_n \sin nx \sinh ny + q_1\eta^c(x, y) + q_2\gamma^c(x, y). \end{aligned}$$

The functions  $\eta(x, y)$  and  $\gamma(x, y)$  are harmonic inside the solution domain and have singular behavior at the transition point between Dirichlet and Robin thermal boundary conditions. They are chosen in accordance with the results of [29], in order to accommodate the discontinuities occurring in the first and the second derivatives of temperature. The concrete forms of these functions, together with their harmonic conjugates  $\eta^c(x, y)$  and  $\gamma^c(x, y)$ , will be introduced later on.

$$\begin{aligned} \phi = & A + a_0 x + b_0 y + c_0 xy + d_0(x^2 - y^2) + \sum_{n=1}^{\infty} a_n \cos nx \cosh ny + \sum_{n=1}^{\infty} b_n \cos nx \sinh ny \\ & + \sum_{n=1}^{\infty} c_n \sin nx \cosh ny + \sum_{n=1}^{\infty} d_n \sin nx \sinh ny, \end{aligned} \quad (13)$$

$$\begin{aligned} \phi^c = & B - b_0 x + a_0 y + 2d_0 xy - \frac{1}{2}c_0(x^2 - y^2) + \sum_{n=1}^{\infty} d_n \cos nx \cosh ny + \sum_{n=1}^{\infty} c_n \cos nx \sinh ny \\ & - \sum_{n=1}^{\infty} b_n \sin nx \cosh ny - \sum_{n=1}^{\infty} a_n \sin nx \sinh ny, \end{aligned} \quad (14)$$

$$\begin{aligned} \psi = & C + f_0 x + g_0 y + h_0 xy + k_0(x^2 - y^2) + \sum_{n=1}^{\infty} f_n \cos nx \cosh ny + \sum_{n=1}^{\infty} g_n \cos nx \sinh ny \\ & + \sum_{n=1}^{\infty} h_n \sin nx \cosh ny + \sum_{n=1}^{\infty} k_n \sin nx \sinh ny + Q_1 \psi_1^S(x, y) + Q_2 \psi_2^S(x, y), \end{aligned} \quad (15)$$

where  $\psi_1^S$  and  $\psi_2^S$  are adequately chosen harmonic functions, each with a singular behavior at one transition point of the mechanical boundary conditions. All the coefficients appearing in the above equations, as well as the form of the singular functions  $\psi_1^S$  and  $\psi_2^S$ , will be determined in the process of the solution. Boundary collocation is used to this end.

## 6 Numerical treatment

The numerical treatment proceeds in two stages:

- Having transformed all the basic equations and conditions into boundary integral equations by means of the boundary integral representation of harmonic functions, these equations are then discretized by dividing the complete angle  $2\pi$  equally into a sufficiently large number  $p$  of sections and placing the same number of nodes on the boundary. These nodes are denoted  $Q_i$  ( $i = 1, 2, \dots, p$ ). As a consequence, the contour  $C$  is approximated to a broken closed contour with unequal side lengths  $\Delta s_i$  ( $i = 1, 2, \dots, p$ ). The transition points are excluded from the set of nodes, in order to avoid the computational errors resulting from the singularities. Any contour integration on  $C$  of a function  $f$  is approximated by a finite sum by the straightforward definition of integration, thus keeping the numerical complexity to a minimum:

$$\oint_C f ds = \sum_{i=1}^p f_i \Delta s_i.$$

The key discretization is that for the boundary integral representation of a harmonic function  $f$  on the contour  $C$ . It reads:

$$f_i = \frac{1}{\pi} \sum_{j=1}^p \left( f_j \frac{\partial \ln R_{ij}}{\partial n_j} + (f_j^c - f_i^c) \frac{\partial \ln R_{ij}}{\partial \tau_j} \right) \Delta s_j, \quad i = 1, 2, \dots, p. \quad (16)$$



The derivative of a function along  $C$  is denoted by a “dot” placed above the symbol of the function, and are calculated numerically. The singularities due to logarithmic terms in the boundary integrals are of removable type. They can be taken care of by considering the following two remarks:

$$\lim_{j \rightarrow i} \left( f_j \frac{\partial \ln R_{ij}}{\partial n_j} \right) = \frac{(\ddot{y}_i \dot{x}_i - \dot{x}_i \dot{y}_i)}{2\omega_i^3} f_i,$$

$$\lim_{j \rightarrow i} \left( (f_j^c - f_i^c) \frac{\partial \ln R_{ij}}{\partial \tau_j} \right) = \frac{1}{\omega_i} \dot{f}_i^c.$$

Details concerning the numerical calculation of derivatives and the removable singularities may be found elsewhere (cf. [7,54,68]). After discretization of all the basic equations and conditions, a linear rectangular algebraic system of equations is obtained for the boundary values of the unknown functions at  $p$  boundary nodes  $Q_i$ . The total number of algebraic equations to be dealt with is  $9p + 9$ , consisting of

1.  $6p$  equations arising from the harmonic representation of the unknown values of the six functions  $T, T^c, \phi, \phi^c, \psi$ , and  $\psi^c$  at  $p$  boundary nodes  $Q_i$ .
2.  $3p$  equations arising from the thermal and the mechanical boundary conditions imposed on the problem under consideration, taken at  $p$  boundary nodes  $Q_i$ .
3. 3 equations, to be applied only in the case of the first fundamental problem of elasticity, arising from the elimination of the rigid body motion.
4. 4 equations arising from the additional simplifying conditions mentioned above.
5. 2 equations arising from: (i) the specification of the value of the conjugate function  $T^c$  at an arbitrarily chosen point and (ii) the specification of the value of the solution at an arbitrarily point for Neumann thermal problem only, due to non-uniqueness of solution for this problem.

The number of unknowns is

1.  $6p$  unknowns representing the values of six functions  $T, T^c, \phi, \phi^c, \psi$  and  $\psi^c$  at  $p$  boundary nodes  $Q_i$ .
2.  $2p$  unknowns representing the values of: (i) the normal and the tangential stress components at nodes on the left half of the boundary for the first subproblem; (ii) two displacement components at nodes on the right half of the boundary for the second subproblem.

One is finally left with a system of  $9p + 9$  linear algebraic equations in  $8p$  unknowns

$$\sum_{n=1}^N A_{mn} X_n = B_m, \quad m = 1, 2, \dots, M, \tag{17}$$

with  $M = 9p + 9$  and  $N = 8p$ . It is thus clear that the resulting system of linear algebraic equations is rectangular. This is resolved by Least Squares. Any obtained solution is substituted back into the system of equations, and the resulting maximal error in satisfying the system is noted. As work is carried out within the frame of uncoupled thermoelasticity, the thermal problem may be resolved independently at first, its solution being subsequently fed into the mechanical problem. This thermal problem is reduced to a system of  $3p + 2$  linear algebraic equations involving  $2p$  unknowns.

- Relying on the obtained results, a boundary analysis is carried out for the mechanical problem in order to assess the effect of the assumed singularities at the transition points, and to infer the type of behavior of the different stress components at these points. As noted earlier, the thermal problem was resolved using singular functions derived elsewhere. Confining our considerations to the mechanical problem, we are interested in the type of singular function  $\psi^S$  to be added to the expression (15) for  $\psi$  will be determined, thus providing an approximate, analytical solution to the problem. Because of the inherent relations between this function and the stress components, we have constructed in Appendix 3, a harmonic function with singular behavior of the second derivatives at a boundary point. A careful analysis of this function has revealed a logarithmic behavior in

its expression. Boundary collocation is now used to find the coefficients of the expansions (13)–(15) of the basic functions inside the cross-sectional domain. After choosing a number of nodes  $S_r \equiv (x_r, y_r)$  ( $r = 1, 2, \dots, R$ ) at proper locations on the boundary, the governing equations and conditions written at these nodes provide a rectangular system of linear algebraic equations for the expansion coefficients. This is solved using Least Squares. The locations of the nodes were simply chosen to correspond to equal increments of the running angular parameter describing the boundary. The number of nodes, however, was varied to achieve the best results. Again, the obtained solutions of the resulting system of equations was substituted back into the system, and the resulting maximal error in satisfying the equations was noted. Expressing the set of equations involving the unknown functions  $\phi$ ,  $\phi^c$  and  $\psi$  symbolically as

$$L(\phi(x, y), \phi^c(x, y), \psi(x, y)) = W(x, y), \quad (18)$$

and substituting the expansions (13)–(15) at the nodes yields a system of equations of the form

$$L(\phi(x_r, y_r), \phi^c(x_r, y_r), \psi(x_r, y_r)) = W(x_r, y_r), \quad r = 1, 2, \dots, R. \quad (19)$$

in the expansion coefficients. Unlike the previous system, the present one can be made square by properly choosing the number of terms in the above expansions, and the number of nodes entering in the collocation procedure. Numerous computational experiments were carried out to reach the best results. In the above-mentioned procedure, we did not come across the question of determining the condition number of the systems of equations appearing during the intermediate steps of the solution. Alternatively, our attention was focused on estimating the error in satisfying the boundary conditions of the problem under consideration.

## 7 Numerical results

A system of orthogonal Cartesian coordinates is used, with origin 0 at the center of the square, and  $x$ -axis perpendicular to the curved side of the square. The boundary conditions are represented in Fig. 1. The side carrying Robin's thermal boundary condition is opposite to the curved side of the square. Such a configuration allows using previously obtained results for the heat problem. The contour is expressed parametrically in terms of a running angular parameter  $\theta$  as follows:

$$x(\theta) = \begin{cases} a - h \left( a + \frac{a}{\Theta} \theta \right)^2 \left( 1 - \left( a + \frac{a}{\Theta} \theta \right) \right)^2, & 0 \leq \theta \leq \Theta, \\ a \cot \theta, & \Theta \leq \theta \leq \pi - \Theta, \\ -a, & \pi - \Theta \leq \theta \leq \Theta + \pi, \\ -a \cot \theta, & \Theta + \pi \leq \theta \leq 2\pi - \Theta, \\ a - h \left( a + \frac{a}{\Theta} (\theta - 2\pi) \right)^2 \left( 1 - \left( a + \frac{a}{\Theta} (\theta - 2\pi) \right) \right)^2, & 2\pi - \Theta \leq \theta \leq 2\pi, \end{cases}$$

$$y(\theta) = \begin{cases} \frac{a}{\Theta} \theta, & 0 \leq \theta \leq \Theta, \\ a, & \Theta \leq \theta \leq \pi - \Theta, \\ -a \tan \theta, & \pi - \Theta \leq \theta \leq \Theta + \pi, \\ -a, & \Theta + \pi \leq \theta \leq 2\pi - \Theta, \\ \frac{a}{\Theta} (\theta - 2\pi), & 2\pi - \Theta \leq \theta \leq 2\pi, \end{cases}$$

with  $\Theta = \pi/4$ ,  $2a$  the side length of the complete square, and  $\theta$  denotes the polar angle of a general point on the truncated boundary. For dimensional analysis purposes, one takes  $a = 1/2$ .

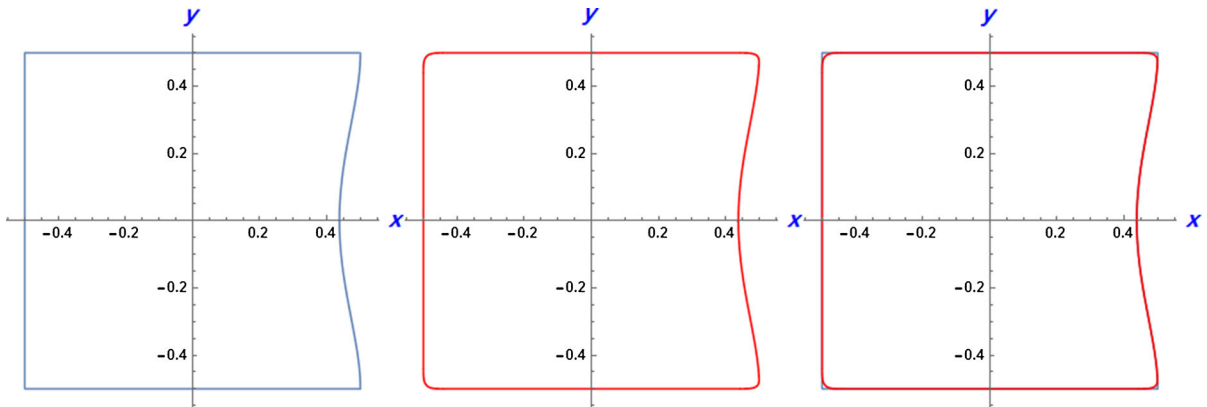


**Fig. 2** Boundary: original, smoothed and comparison

This boundary belongs to the class  $C^0$  and consequently does not satisfy the smoothness condition necessary for an efficient performance of the present approach. A smoothing process by Fourier series is undertaken at the corners to achieve a new boundary close to the original one and belonging to the class  $C^2$  **at least**. The cross-section for which the present results is obtained is shown in Fig. 2 for  $h = 1.0$ .

It is worth noting that within the presented numerical scheme a closer approximation to the original square boundary will result in larger errors in satisfying the boundary conditions of the problem.

The boundary of the domain is subjected to the following boundary conditions:

*Thermal conditions*

- Neumann type

$$\frac{\partial T}{\partial n} = 0 \text{ for } y = -a, -a \leq x \leq a \text{ and } x = a - h(a + y)^2(1 - a - y)^2, -a \leq y \leq a,$$

- Dirichlet type

$$T = 0 \text{ for } y = a, -a \leq x \leq a,$$

- Robin type

$$-\frac{\partial T}{\partial x} + Bi(T - 1) = 0 \text{ for } x = -a, -a \leq y \leq a,$$

with Biot constant  $Bi = 0.1$ .

A steady temperature field is established in the rectangle due to heat inflow through the left boundary and heat outflow through the upper boundary.

*Mechanical conditions*

- The right half of the boundary is subjected to a tension of intensity  $p$  given by:

$$p(\theta) = h_2 \cos^8 \theta, \quad 0 \leq \theta < \theta_1 \text{ and } \theta_2 < \theta \leq 2\pi, \tag{20}$$

and  $h_2 = 0.1$ . This choice makes the tension distribution tend to zero smoothly enough at both ends of its interval of definition. Stiffer choices for the applied tension is bound to increase the computational errors.

- The left half of the boundary is completely fixed,

$$u = 0, \quad v = 0, \quad \theta_1 \leq \theta \leq \theta_2, \quad (21)$$

where

$$\theta_1 = \frac{\pi}{2}, \quad \theta_2 = \frac{3\pi}{2}.$$

The harmonic functions  $\eta(x, y)$  and  $\gamma(x, y)$  appearing in the expression for temperature, and their harmonic conjugates have been proposed by Abou-Dina and Ghaleb [29] to deal with the weak singularities of temperature at the upper left corner of the square. They are given as:

$$\begin{aligned} \eta(x, y) &= -\frac{2Bi}{\pi} \left[ \rho(x, y) \cos(\zeta(x, y)) \ln(\rho(x, y)) - \zeta(x, y) \rho(x, y) \sin(\zeta(x, y)) \right], \\ \gamma(x, y) &= -\frac{Bi^2}{\pi} \left[ \rho^2(x, y) \ln(\rho(x, y)) \sin(2\zeta(x, y)) + \rho^2(x, y) \zeta(x, y) \cos(2\zeta(x, y)) \right], \\ \eta^c(x, y) &= -\frac{2Bi}{\pi} \left[ \rho(x, y) \ln(\rho(x, y)) \sin(\zeta(x, y)) + \rho(x, y) \zeta(x, y) \cos(\zeta(x, y)) \right], \\ \gamma^c(x, y) &= \frac{Bi^2}{\pi} \left[ \rho^2(x, y) \ln(\rho(x, y)) \cos(2\zeta(x, y)) - \rho^2(x, y) \eta(x, y) \sin(2\zeta(x, y)) \right]. \end{aligned}$$

The variables  $(\rho, \zeta)$  denote a local system of polar coordinates centered at the upper left corner  $(-a, a)$ , and polar axis directed along the left side of the square. Thus,

$$\begin{aligned} \rho(x, y) &= \sqrt{(0.50 + x)^2 + (0.50 - y)^2}, \\ \zeta(x, y) &= \tan^{-1} \left( \frac{0.50 - y}{0.50 + x} \right). \end{aligned}$$

Boundary collocation is used to find the values of temperature inside the domain. According to this method, expressions involving the unknown harmonic functions are set equal to their values at some chosen boundary nodes. As a result, a set of linear algebraic equations is obtained for the coefficients appearing in these expressions. As noted earlier, the nodes are placed at equal increments of the running angular parameter describing the boundary. Their number is allowed to vary for best results. To calculate the temperature displacements  $u_T$  and  $v_T$ , the point  $M_0$  is taken at the center of the square, i.e., at the origin of coordinates. The integrations in (10) are easily performed on paths formed by segments parallel to the coordinate axes. The resulting expressions have no specific symmetry with respect to the coordinate axes due to the type of used thermal boundary conditions. The mechanical problem is replaced by two subproblems, one with given stresses, and the other with given displacements on the boundary, having a common solution (cf. [54]). This configuration is represented in Fig. 3.

As noted earlier, for each of these two subproblems, the boundary conditions are given on one part of the boundary and complemented with unknown values on the other part, to be determined as part of the solution. Following [67], the equations for each of these two subproblems are reduced to a rectangular system of boundary integral equations with the use of the boundary integral representation of harmonic functions. This system is then discretized as explained above. The singular behavior of the stress components at the two separation boundary points is put in evidence and a singular solution is added to the basic harmonic function  $\psi$  to find the solution inside the cross-sectional domain in the form of expansions. The coefficients in these expansions are determined by the boundary collocation. Plots are given for the unknown functions on the boundary and in the bulk. The efficiency of the used numerical scheme is discussed. All the figures were produced using Mathematica 9.0 software.

Although there is symmetry with respect to the  $x$ -axis of the transition points and the mechanical boundary conditions, it is worth noting that the solutions for the basic unknown functions have no specific symmetry with

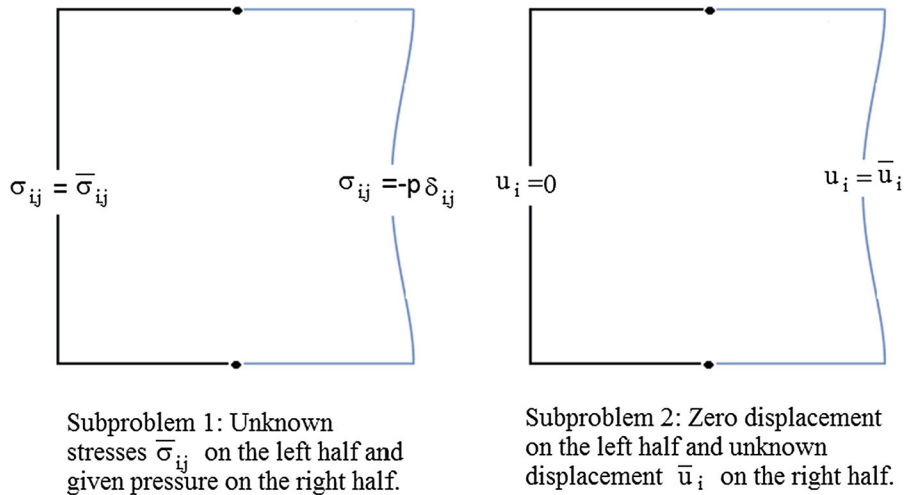


Fig. 3 Two subproblems

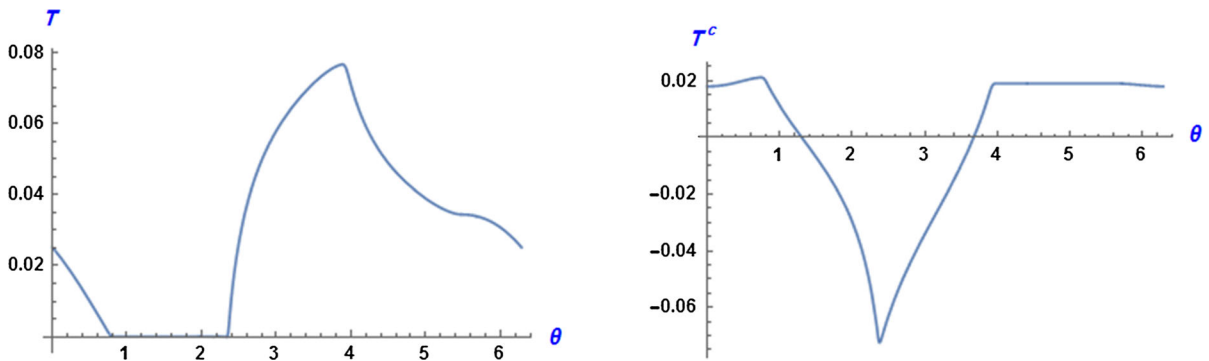


Fig. 4 Temperature  $T$  and its conjugate  $T^c$  on the boundary

respect to the axes of coordinates. This is due to the lack of symmetry of the temperature displacements  $u_T$  and  $v_T$  entering in the boundary conditions.

No analytical solution for this problem is available for comparison. The following figures show the optimal results obtained with 217 nodal points for the boundary integral formulation. Optimality in this context means fewer fluctuations, more regular curves, and the least errors in satisfying the boundary conditions. Many computational experiments were carried out in order to find the best truncation of the expansions. It was found that 65 terms in the expansions for the basic harmonic functions  $\phi$ ,  $\phi^c$ ,  $\psi$ , and  $\psi^c$  yield optimal results. All systems of equations were solved using Least Squares. After a solution is obtained, it is substituted back into the equations for error analysis. The errors were less than  $12 \times 10^{-4}$  in satisfying the imposed boundary conditions, while for the determination of the expansion coefficients, the maximum error in satisfying the system of equations did not exceed  $11 \times 10^{-3}$ . The seemingly large number of terms in the expansions is due, in our opinion, to the effect of the singular behavior of the stress components at the transition points.

Figure 5 shows the boundary displacement due to temperature only. Such displacement is not bound to satisfy any boundary conditions.

The boundary analysis clearly indicates some kind of discontinuity occurring in the stress components at the boundary transition points. Based on this observation, the expansion of the basic harmonic function  $\psi$  has been enriched with an additional term involving a harmonic function that has a singular boundary behavior at the separation points. More precisely, this function has discontinuous second order derivatives at a boundary point.

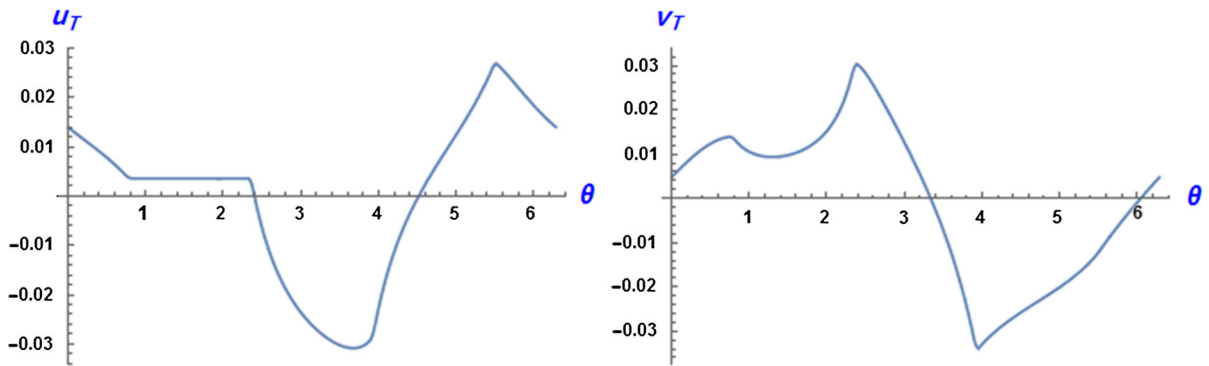


Fig. 5 Temperature displacements  $u_T$  and  $v_T$  on the boundary

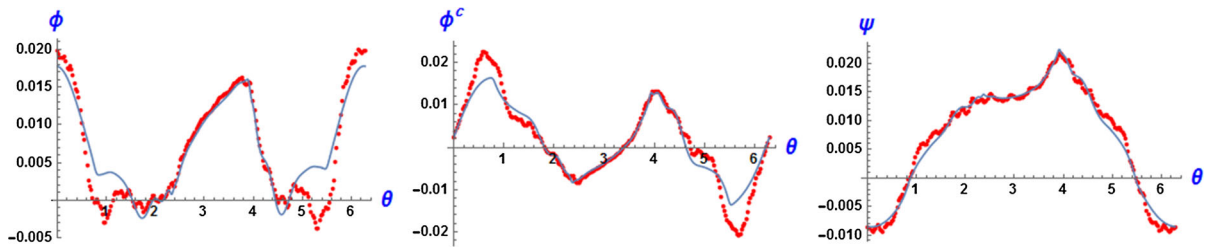


Fig. 6 The harmonic functions on the boundary

Fig. 7 Stress function on the boundary

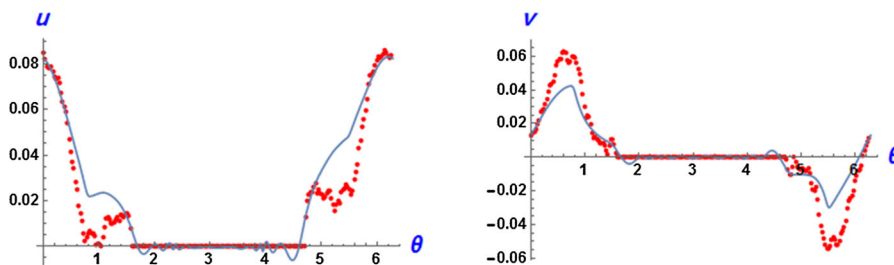
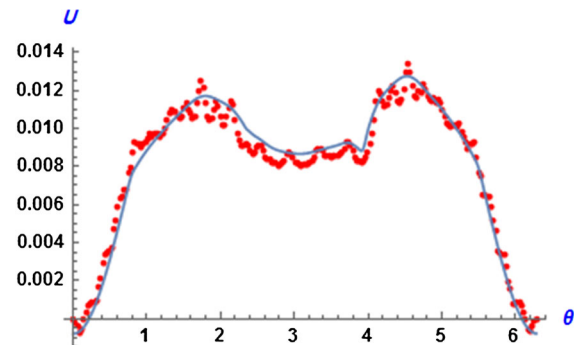


Fig. 8 Displacement on the boundary

The steps for building such a function are presented in Appendix 3. The stresses resulting from this function as stress function are shown in Fig. 19. The plots in Figs. 4, 5, 6, 7, 8, 9 and 10 show the values of the basic unknown functions as calculated from the boundary analysis (dotted curves), together with the values of these functions as obtained from the expansions (line curves). Good agreement is reached.

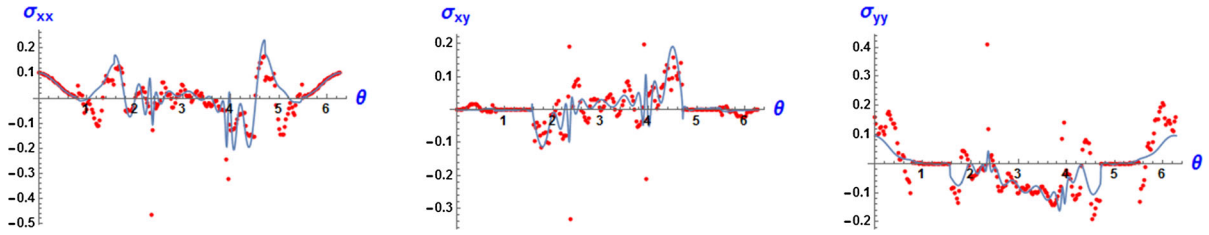


Fig. 9 Components of the stress tensor on the boundary

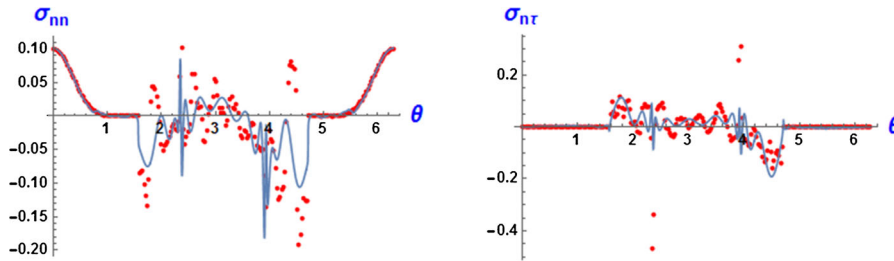


Fig. 10 Tangential and normal components of the stress tensor on C

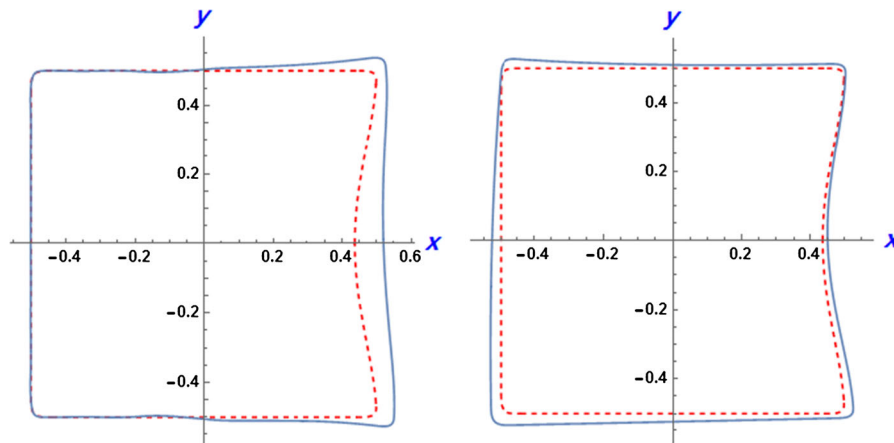
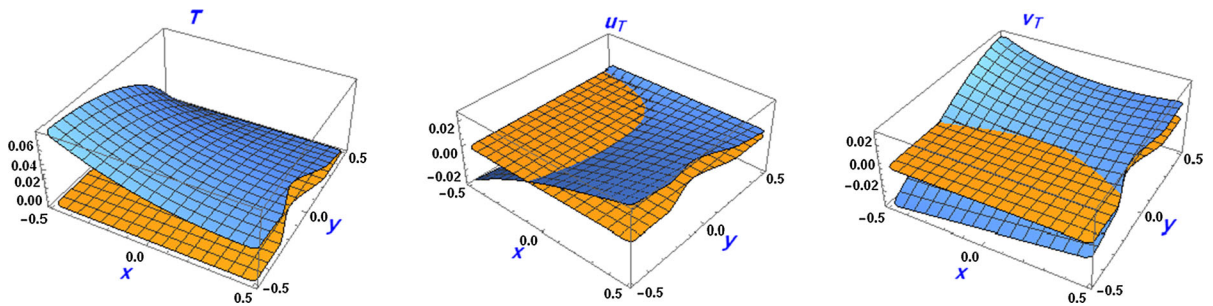
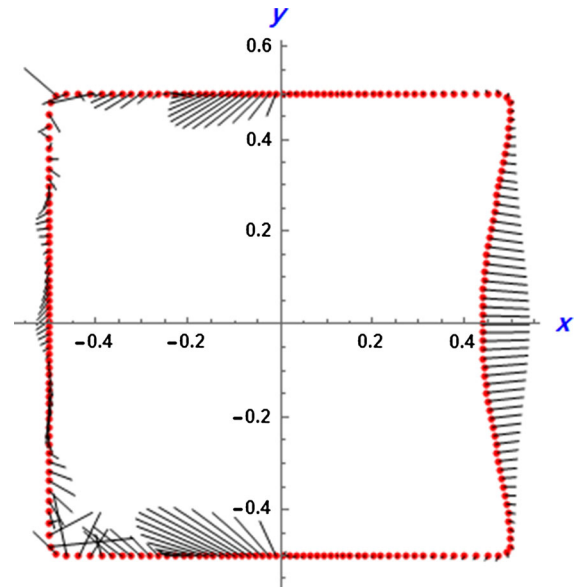


Fig. 11 Total displacement (left) and temperature displacement (right). The original boundary is shown for comparison (dashed curve)

The deformed contour showing the combined action of external mechanical and thermal factors is represented in the left in Fig. 11. One notes here the fulfillment of the partial fixing of the boundary. The right part of this same figure shows the boundary displacement due to temperature alone, i.e., the effect of the temperature displacements  $u_T$  and  $v_T$ .

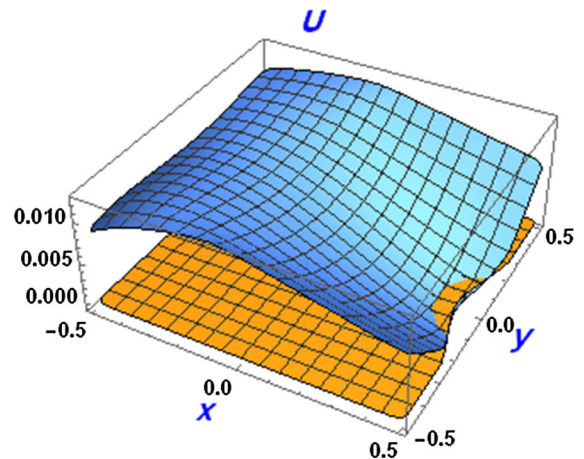
The boundary distribution of the stress vector is represented in Fig. 12 in magnitude and direction. It is worth noting that this vector is directed outwards the cross-section everywhere on the right half of the boundary as expected, while it is directed inwards on the left (fixed) half. There are two locations close to the separation points, and two other locations at the left corners of the cross-section, where the stress vector attains relatively large values. It is at these locations that a detachment of the boundary can potentially take place. The corresponding emplacements can be noticed on the curves for the normal and the tangential components of stress obtained from boundary analysis (dotted curves) in Fig. 10. The discontinuities of the stress vector appearing at the two left corners may be attributed to the sharp change in direction of the normal to the boundary at these points.

**Fig. 12** Stress vector distribution on the boundary



**Fig. 13**  $T(x, y)$ ,  $u_T(x, y)$  and  $v_T(x, y)$

**Fig. 14**  $U(x, y)$



The distributions of functions of practical interest inside the cross-sectional domain are shown in 3-D in Figs. 13, 14, 15 and 16. The cross-sectional domain over which these functions are plotted is also shown in these figures for convenience.



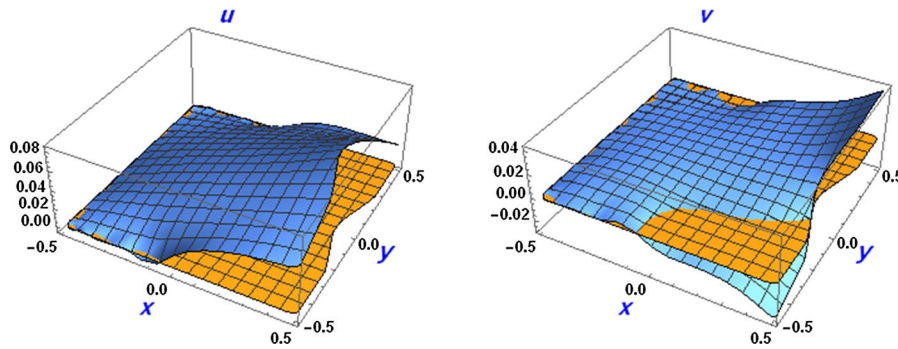


**Fig. 15**  $u(x, y)$  and  $v(x, y)$

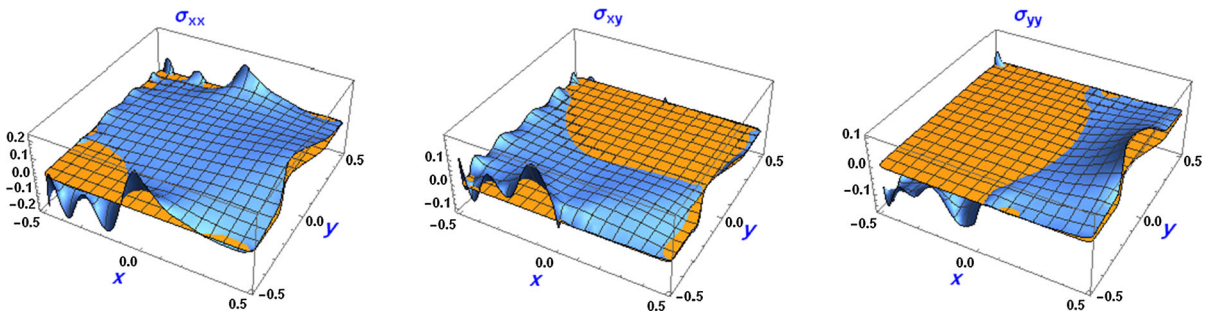


**Fig. 16**  $\sigma_{xx}(x, y)$ ,  $\sigma_{xy}(x, y)$  and  $\sigma_{yy}(x, y)$

## 8 Conclusions

A boundary integral method has been used to solve the plane problem of linear, uncoupled thermoelasticity for a square domain under mixed thermal and mechanical conditions, with one part of the boundary fixed, the other subjected to a variable tension. No solution is available for this problem in the literature. In essence, the proposed solution method is similar in nature to those existing in the literature, but the technique is different. It consists of using two different approaches to find the solution: a boundary analysis relying on the boundary integral representation of harmonic functions and boundary collocation with an expansion of the unknown basic harmonic functions in a series of polar harmonics. The unknown functions are obtained on the boundary and inside the domain of the normal cross-section. The weak singularities of the stress function arising at the transition points of the mechanical boundary conditions have been treated by introducing a harmonic function with singular behavior at these points. The way to construct such a function is explained. The boundary corner effects were removed by smoothing using polynomials (cf. [59]) in order to reduce computational errors.

For the present choices of the different parameters, the errors occurring within the boundary analysis do not exceed  $1 \times 10^{-2}$ . Inside the domain, the unknown functions were expanded in terms of harmonic functions. The boundary collocation method was used to find the coefficients. A relatively large number of terms (65 terms) in the expansions was necessary to reach acceptable errors that satisfy the mechanical mixed boundary conditions. This is an expression of the singular behavior of the solution at the transition points. The deformations of the boundary due to heat effect alone and due to the combined thermomechanical action are displayed. The results indicate that potential debonding of the fixed part of the boundary may occur near the transition points or at the fixed corners. The same method could be applied to other types of thermal or mechanical boundary conditions. The form of the singular function has to be found separately for each case. It is believed that the present investigation may be of interest in evaluating the stresses in long pad supports under mechanical loads and thermal action, when both factors are important.

## Appendix 1: Boundary representation of harmonic functions

For an arbitrary point  $(x, y) \in D$ , the boundary integral representation of harmonic functions reads:

$$f(x, y) = \frac{1}{2\pi} \oint_C \left( f \frac{\partial \ln R}{\partial n'} - \ln R \frac{\partial f}{\partial n'} \right) ds'.$$

Here  $R$  is the distance between the point  $(x, y)$  and the current integration point. When the point  $(x, y)$  tends to a boundary point, this relation transforms into an integral equation for the boundary values of the function  $f$ . Using integration by parts, this may be rewritten as

$$f(x, y) = \frac{1}{\pi} \oint_C \left( f(x', y') \frac{\partial \ln R}{\partial n'} + (f^c(x', y') - f^c(x, y)) \frac{\partial \ln R}{\partial \tau'} \right) ds',$$

where  $(x', y')$  is the current integration point.

This last equation contains removable singularities, which can be treated as explained in [67].

## Appendix 2: The first and second derivatives of harmonic functions with respect to $x$ and $y$ on the boundary

For a general harmonic function  $f$  in the cross section, the following formulas are used:

$$\begin{aligned} \left. \frac{\partial f}{\partial x} \right|_i &= \frac{1}{\omega_i^2} (\dot{f}_i^c \dot{y}_i + \dot{f}_i \dot{x}_i), \\ \left. \frac{\partial f}{\partial y} \right|_i &= \frac{1}{\omega_i^2} (\dot{f}_i \dot{y}_i - \dot{f}_i^c \dot{x}_i), \\ \left. \frac{\partial^2 f}{\partial y^2} \right|_i &= \frac{\alpha_i}{\omega_i^4} \ddot{f}_i - \frac{\beta_i}{\omega_i^4} \ddot{f}_i^c + \frac{\rho_i}{\omega_i^6} \dot{f}_i + \frac{\rho_i}{\omega_i^6} \dot{f}_i^c, \\ \left. \frac{\partial^2 f}{\partial x \partial y} \right|_i &= \frac{\beta_i}{\omega_i^4} \ddot{f}_i + \frac{\alpha_i}{\omega_i^4} \ddot{f}_i^c - \frac{\rho_i}{\omega_i^6} \dot{f}_i - \frac{\rho_i}{\omega_i^6} \dot{f}_i^c, \\ \left. \frac{\partial^2 f}{\partial x^2} \right|_i &= -\frac{\alpha_i}{\omega_i^4} \ddot{f}_i + \frac{\beta_i}{\omega_i^4} \ddot{f}_i^c + \frac{\rho_i}{\omega_i^6} \dot{f}_i - \frac{\rho_i}{\omega_i^6} \dot{f}_i^c, \end{aligned}$$

where  $f$  stands for any one of the used harmonic functions, and

$$\begin{aligned} \rho_i &= \alpha_i \gamma_i + \beta_i \delta_i, \\ \rho_i &= \alpha_i \delta_i - \beta_i \gamma_i, \end{aligned}$$

with

$$\begin{aligned} \alpha_i &= \dot{y}_i^2 - \dot{x}_i^2, \\ \beta_i &= 2 \dot{x}_i \dot{y}_i, \\ \gamma_i &= \dot{x}_i \ddot{y}_i - \dot{y}_i \ddot{x}_i, \\ \delta_i &= \dot{x}_i \ddot{x}_i + \dot{y}_i \ddot{y}_i. \end{aligned}$$

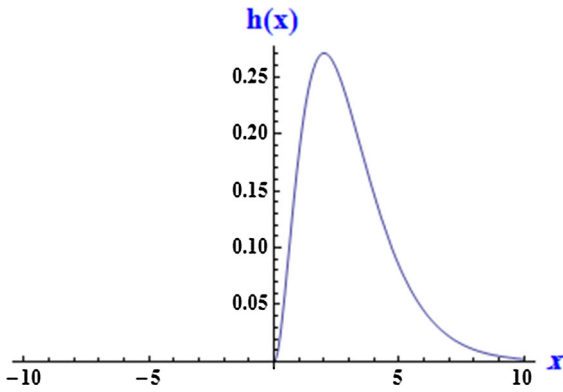


Fig. 17 The function  $h(x)$

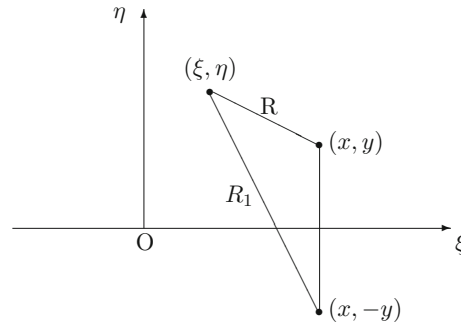


Fig. 18 Green's function technique

### Appendix 3: Treating the stress singularities

In order to simulate the singular behaviours of stresses at the two boundary points of contact, we have proceeded according to the following scheme:

1. Our goal is to introduce a harmonic function that has weak singularities at a boundary point, more precisely a harmonic function that has discontinuous second derivatives at a boundary point.
2. Let  $h(x)$  be a function of the real variable  $x$  defined on the real axis, such that it is continuous with a continuous derivative everywhere, but has a finite jump in the second derivative at the point  $x = 0$ . Let this function be of the form:

$$h(x) = \begin{cases} 0 & x \leq 0, \\ \frac{1}{2}x^2 e^{-x} & x > 0. \end{cases}$$

The exponential function is needed here to make the function integrable on the real axis. The graph of this function is shown in Fig. 17.

3. The boundary integral representation of harmonic functions applied to a function  $f$  which is harmonic in a simply connected domain  $D$  bounded by a smooth surface  $S$  yields

$$f(x, y) = \oint_S \left[ f \frac{\partial}{\partial n'} \left( \frac{1}{2\pi} \ln R \right) - \left( \frac{1}{2\pi} \ln R \right) \frac{\partial}{\partial n'} f \right] ds', \tag{22}$$

where  $(x, y)$  is an arbitrary point in  $D$ ,  $n'$  denotes the outward unit normal to  $S$  at the integration point, and  $R$  is the distance function between the point  $(x, y)$  and the integration point.

If  $D$  is the upper half-plane  $(\xi, \eta)$ ,  $\eta > 0$ , the previous equation takes the form:

$$f(x, y) = - \int_{-\infty}^{+\infty} \left[ f \frac{\partial}{\partial \eta} \left( \frac{1}{2\pi} \ln R \right) - \left( \frac{1}{2\pi} \ln R \right) \frac{\partial}{\partial \eta} f \right] d\xi. \tag{23}$$

Let  $R_1$  be the distance shown in Fig. 18. The function  $\ln R_1$  is harmonic on the upper half-plane. A well-known theorem of the Theory of Potential, applied to the harmonic functions  $f$  and  $\ln R_1$ , yields

$$0 = \int_{-\infty}^{+\infty} \left[ f \frac{\partial}{\partial \eta} \left( \frac{1}{2\pi} \ln R_1 \right) - \left( \frac{1}{2\pi} \ln R_1 \right) \frac{\partial}{\partial \eta} f \right] d\xi. \tag{24}$$

Adding and noting that  $R = R_1$  on the  $\xi$ -axis, one gets

$$\begin{aligned} f(x, y) &= - \int_{-\infty}^{+\infty} \left[ f \frac{\partial}{\partial \eta} \left( \frac{1}{2\pi} \ln R - \frac{1}{2\pi} \ln R_1 \right) \right] d\xi \\ &= \int_{-\infty}^{+\infty} \left[ f \frac{\partial}{\partial \eta} \left( \frac{1}{2\pi} \ln \frac{1}{R} - \frac{1}{2\pi} \ln \frac{1}{R_1} \right) \right] d\xi. \end{aligned}$$

The function under the normal derivative in the last equation is just Green's function for the Dirichlet problem in the upper half-plane:

$$\begin{aligned} G(\xi, \eta; x, y) &= \frac{1}{2\pi} \ln \frac{1}{R} - \frac{1}{2\pi} \ln \frac{1}{R_1} \\ &= \frac{1}{2\pi} \ln \frac{R_1}{R}. \end{aligned}$$

One has

$$\begin{aligned} \frac{\partial G}{\partial \eta} &= \frac{1}{2\pi} \frac{\partial}{\partial \eta} \ln \frac{R_1}{R} \\ &= \frac{1}{4\pi} \frac{\partial}{\partial \eta} \ln \frac{(\xi - x)^2 + (\eta + y)^2}{(\xi - x)^2 + (\eta - y)^2} \\ &= \frac{1}{2\pi} \frac{(\xi - x)^2 + (\eta - y)^2}{(\xi - x)^2 + (\eta + y)^2} \frac{[(\xi - x)^2 + (\eta - y)^2] - (\eta - y)[(\xi - x)^2 + (\eta + y)^2]}{[(\xi - x)^2 + (\eta - y)^2]^2}. \end{aligned}$$

Thus,

$$\left. \frac{\partial G}{\partial \eta} \right|_{\eta=0} = \frac{1}{2\pi} \frac{2y}{(\xi - x)^2 + y^2}.$$

and the function  $f$  takes the form:

$$f(x, y) = \frac{1}{2\pi} \int_{-\infty}^{+\infty} h(\xi) \frac{2y}{(\xi - x)^2 + y^2} d\xi \quad (25)$$

$$= \frac{1}{2\pi} \int_0^{+\infty} \xi^2 e^{-\xi} \frac{y}{(\xi - x)^2 + y^2} d\xi. \quad (26)$$

4. In order to perform the integration, we write

$$\frac{\xi^2}{(\xi - x)^2 + y^2} = \frac{\xi^2}{\xi^2 - 2x\xi + x^2 + y^2} = \frac{\xi^2}{(\xi + c_1)(\xi + c_2)}, \quad (27)$$

where

$$c_1 = -x + iy, \quad c_2 = -x - iy = \bar{c}_1 \quad (28)$$

and “bar” denotes the conjugate. Expansion in partial fractions yields after some manipulations:

$$\frac{\xi^2}{(\xi - x)^2 + y^2} = 1 - \frac{c_1^2}{2iy} \frac{1}{\xi + c_1} + \frac{c_2^2}{2iy} \frac{1}{\xi + c_2}. \quad (29)$$

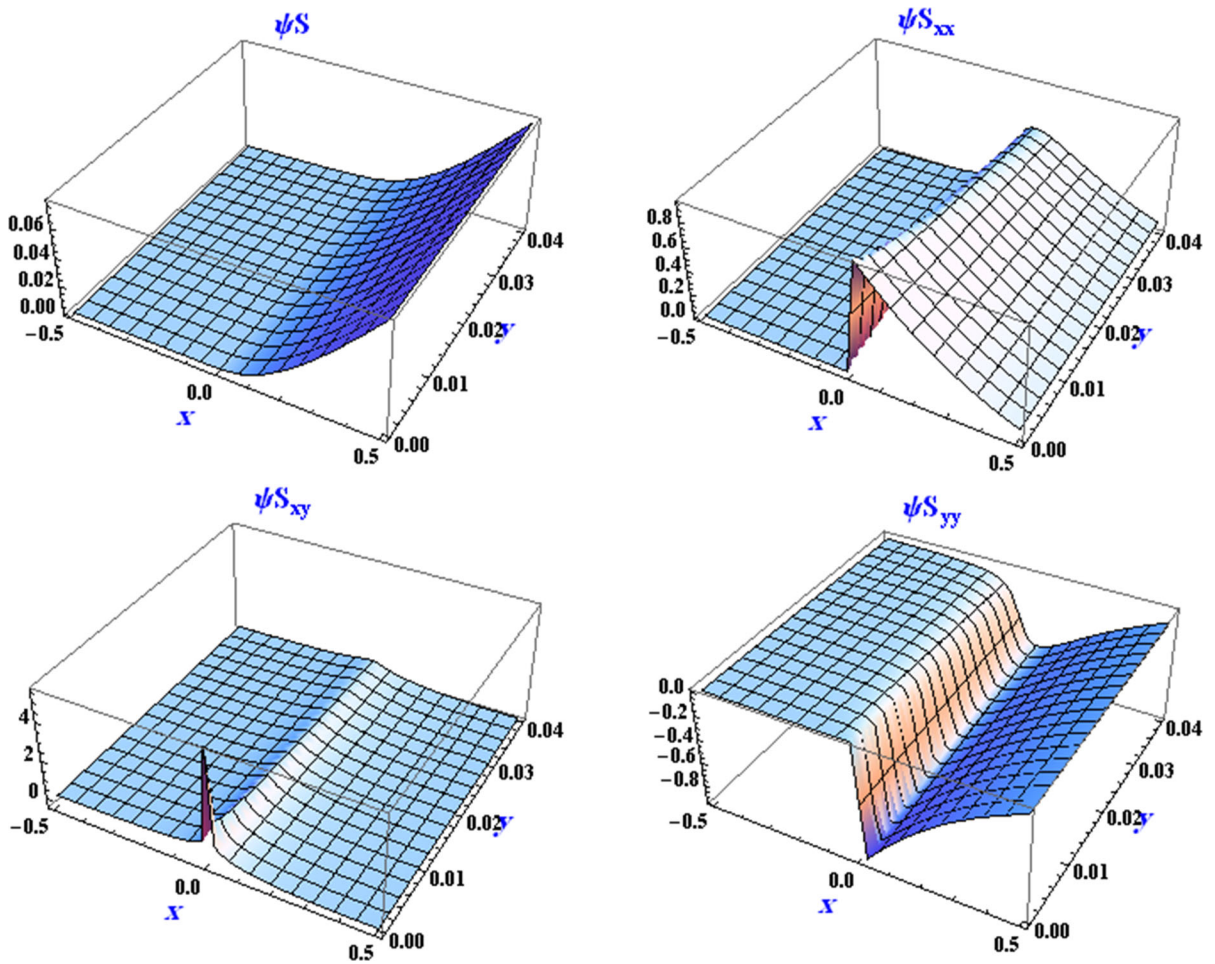


Fig. 19 Singular stresses

Hence,

$$f(x, y) = \frac{1}{2\pi} \int_0^{+\infty} \left[ y - \frac{c_1^2}{2i} \frac{1}{\xi + c_1} + \frac{c_2^2}{2i} \frac{1}{\xi + c_2} \right] e^{-\xi} d\xi. \tag{30}$$

5. Next, introduce the integral exponential function  $E_1(z)$  of the complex argument  $z$  by the formula ([69, p. 62]):

$$E_1(z) = \int_z^\infty \frac{e^{-t}}{t} dt = e^{-z} \int_0^\infty \frac{e^{-t}}{t+z} dt. \tag{31}$$

One has

$$E_1(z) = -\gamma - \ln(z) - \sum_{n=1}^\infty \frac{(-1)^n z^n}{n n!}, \tag{32}$$

where  $\gamma = 0.5772156649$  is Euler's constant. Finally,

$$f(x, y) = \frac{1}{2\pi} \left[ y + 2\operatorname{Re} \left( \frac{i c_1^2}{2} e^{c_1} E_1(c_1) \right) \right].$$

Substitution for the exponential integral function allows one to compute the function  $f(x, y)$ .

- The obtained function will now be centered at each of the two boundary separation points in order to simulate the behavior of stresses there. The sum of the resulting two functions is now taken to replace the function  $\psi$  in the above formulation, and will be denoted  $\psi_S$ . The three-dimensional plots illustrated in Fig. 19 show the harmonic function with singular boundary behavior, and the singular stresses as calculated from it as the stress function.

## References

- Nowacki W (1962) Thermoelasticity. In: von Kármán T, Deyden HL (eds) International series of monographs on aeronautics and astronautics, division I: solid and structural mechanics, vol 3. Addison-Wesley, Reading
- Ieşan D (2004) Thermoelastic models of continua. In: Gladwell GML (ed) Solid mechanics and its applications, vol 118. Springer, Dordrecht
- Hetnarski RB, Eslami MR (2009) Thermal stresses-advanced theory and applications. Springer, Dordrecht
- Shanker MU, Dhaliwal RS (1972) Singular integral equations in asymmetric thermoelasticity. *J Elast* 2(1):59–71
- Singh BM, Dhaliwal RS (1978) Mixed boundary-value problems of steady-state thermoelasticity and electrostatics. *J Therm Stress* 1(1):1–11
- Abou-Dina MS, Ghaleb AF (2002) On the boundary integral formulation of the plane theory of thermoelasticity. *J Therm Stress* 25(1):1–29
- Abou-Dina MS, El-Seadawy G, Ghaleb AF (2007) On the boundary integral formulation of the plane problem of thermo-elasticity with applications (computational aspects). *J Therm Stress* 30(5):475–503
- El-Dhaba AR, Ghaleb AF, Abou-Dina MS (2003) A problem of plane, uncoupled linear thermoelasticity for an infinite, elliptical cylinder by a boundary integral method. *J Therm Stress* 26(2):93–121
- Hasebe N, Wanga X (2005) Complex variable method for thermal stress problem. *J Therm Stress* 28(6–7):595–648
- Han JJ, Hasebe N (2002) Green's function for thermal stress mixed boundary-value problem of an infinite plane with an arbitrary hole under a point heat source. *J Therm Stress* 25(12):1147–1160
- Şeremet V (2010) New Poisson integral formulas for thermoelastic half-space and other canonical domains. *Eng Anal Bound Elem* 34(2):158–162
- Şeremet V (2010) New explicit Green's functions and Poisson integral formula for a thermoelastic quarter-space. *J Therm Stress* 33(4):356–386
- Şeremet V (2010) Exact elementary Green functions and Poisson-type integral formulas for a thermoelastic half-wedge with applications. *J Therm Stress* 33(12):1156–1187
- Şeremet V (2011) A new technique to derive the Green's type integral formula in thermoelasticity. *Eng Math* 69(4):313–326
- Şeremet V (2011) Deriving exact Green's functions and integral formulas for a thermoelastic wedge. *Eng Anal Bound Elem* 35(3):327–332
- Şeremet V (2012) New closed-form Green's function and integral formula for a thermoelastic quadrant. *Appl Math Model* 36(2):799–812
- Şeremet V (2014) Recent integral representations for thermoelastic Green's functions and many examples of their exact analytical expressions. *J Therm Stress* 37(5):561–584
- Şeremet V, Bonnet G (2011) New closed-form thermoelastostatic Green's function and Poisson-type integral formula for a quarter-plane. *Math Comput Model* 53(1–2):347–358
- Meleshko VV (1995) Equilibrium of elastic rectangle: Mathieu–Inglis–Pickett solution revisited. *J Elast* 40:207–238
- Meleshko VV (1997) Bending of an elastic rectangular clamped plate: exact versus 'engineering' solutions. *J Elast* 48:1–50
- Meleshko VV (2011) Thermal stresses in an elastic rectangle. *J Elast* 105(1–2):61–92
- Chen WQ, Lee KY, Ding HI (2004) General solution for transversely isotropic magneto-electro-thermoelasticity and the potential theory method. *Int J Eng Sci* 42(13–14):1361–1379
- El-Dhaba AR, Ghaleb AF, Abou-Dina MS (2007) A plane problem of uncoupled thermomagnetoelasticity for an infinite, elliptical cylinder carrying a steady axial current by a boundary integral method. *Appl Math Model* 31(3):448–477
- Kupradze DV (1963) Methods of potential in theory of elasticity. Fizmatgiz, Moscow
- Jaswon MA, Symm GT (1977) Integral equation methods in potential theory and elastostatics. Academic Press, London
- Helsing J, Ojala R (2008) On the evaluation of layer potentials close to their sources. *J Comput Phys* 227(5):2899–2921

27. Fairweather G, Karageorghis A (1998) The method of fundamental solutions for elliptic boundary-value problems. *Adv Comput Math* 9:69–95
28. Abou-Dina MS (2002) Implementation of Trefftz method for the solution of some elliptic boundary-value problems. *J Appl Math Comput* 127(1):125–147
29. Abou-Dina MS, Ghaleb AF (2004) A variant of Trefftz's method by boundary Fourier expansion for solving regular and singular plane boundary-value problems. *J Comput Appl Math* 167:363–387
30. Read WW (2007) An analytic series method for Laplacian problems with mixed boundary conditions. *J Comput Appl Math* 209:22–32
31. Haller-Dintelmann R, Kaiser H-C, Rehberg J (2008) Elliptic Dintel problems including mixed boundary conditions. *J Math Pure Appl* 89:25–48
32. Costea N, Firoiu I, Preda FD (2013) Elliptic boundary-value problems with nonsmooth potential and mixed boundary conditions. *J Therm Stress* 58(9):1201–1213
33. El-Dhaba AR, Abou-Dina MS, Ghaleb AF (2015) Deformation for a rectangle by a finite Fourier transform. *J ComputTheor Nanosci* 12:1–7
34. El-Dhaba AR, Abou-Dina MS (2015) Thermal stresses induced by a variable heat source in a rectangle and variable pressure at its boundary by finite Fourier transform. *J Therm Stress* 38:677–700
35. Altiero NJ, Gavazza SD (1980) On a unified boundary-integral equation method. *J Elast* 10(1):1–9
36. Heise U (1980) Systematic compilation of integral equations of the Rizzo type and of Kupradze's functional equations for boundary-value problems of plane elastostatics. *J Elast* 10(1):23–56
37. Heise U (1982) Solution of integral equations for plane elastostatical problems with discontinuously prescribed boundary values. *J Elast* 12(3):293–312
38. Koizumia T, Tsujib T, Takakudac K, Shibuya T, Kurokawad K (1988) Boundary integral equation analysis for steady thermoelastic problems using thermoelastic potential. *J Therm Stress* 11(4):341–352
39. Constanda C (1995) The boundary integral equation method in plane elasticity. *Proc Am Math Soc* 123(11):3385–3396
40. Constanda C (1995) Integral equations of the first kind in plane elasticity. *Q Appl Math Mech Solids* 1:251–260
41. Schiavone P (1996) Integral equation methods in plane asymmetric elasticity. *J Elast* 43(1):31–43
42. Peters G, Helsing J (1998) Integral equation methods and numerical solutions of crack and inclusion problems in planar elastostatics. *Siam J Appl Math* 59(3):965–982
43. Schiavone P (2001) Integral solutions of mixed problem in a theory of plane strain elasticity with microstructure. *Int J Eng Sci* 39:1091–1100
44. Wu X, Li C, Kong W (2006) A Sinc-collocation method with boundary treatment for two-dimensional elliptic boundary value problems. *J Comput Appl Math* 196:58–69
45. Elliotis M, Georgiou G, Xenophontos C (2007) The singular function boundary integral method for biharmonic problems with crack singularities. *Eng Anal Bound Elem* 31:209–215
46. Li Z-C, Chu P-C, Young L-J, Lee M-G (2010) Models of corner and crack singularity of linear elastostatics and their numerical solutions. *Eng Anal Bound Elem* 34:533–548
47. Natroshvili D, Stratis IG, Zazashvili S (2010) Boundary integral equation methods in the theory of elasticity of hemitropic materials: a brief review. *J Comput Appl Math* 234:1622–1630
48. Cheng P, Luo X, Wang Z, Huang J (2012) Mechanical quadrature methods and extrapolation algorithms for boundary integral equations with linear boundary conditions in elasticity. *J Elast* 108(2):193–207
49. Atluri SN, Zhu TL (2002) The meshless local Petrov–Galerkin (MLPG) approach for solving problems in elasto-statics. *J Comput Mech* 25:169–179
50. Rui Z, Jin H, Tao L (2006) Meshless local boundary integral equation method for 2D- elastodynamic problems. *Eng Anal Bound Elem* 30:391–398
51. Sladek J, Sladek V, Van Keer R (2003) Meshless local boundary integral equation method for 2D-elastodynamic problems. *Int J Numer Meth Eng* 57:235–249
52. Helsing J (2009) Integral equation methods for elliptic problems with boundary conditions of mixed type. *J Comput Phys* 228: 8892–8907
53. Khuri MA (2011) Boundary-value problems for mixed type equations and applications. *Nonlinear Anal* 74:6405–6415
54. Gjam AS, Abdusalam HA, Ghaleb AF (2013) Solution for a problem of linear plane elasticity with mixed boundary conditions on an ellipse by the method of boundary integrals. *J Egypt Math Soc* 21(3):361–369
55. Williams ML (1952) Stress singularities resulting from various boundary conditions. *J Appl Mech* 19(4):526–528
56. Haas R, Brauchli H (1992) Extracting singularities of Cauchy integrals—a key point of a fast solver for plane potential problems with mixed boundary conditions. *J Comput Appl Math* 44:167–186
57. Gusenkova AA, Pleshchinskii NB (2000) Integral equations with logarithmic singularities in the kernels of boundary-value problems of plane elasticity theory for regions with a defect. *J Appl Math Mech* 64(3):435–441
58. Kotousov A, Lew YT (2006) Stress singularities resulting from various boundary conditions in angular corners of plates of arbitrary thickness in extension. *Int J Solids Struct* 43(17):5100–5109
59. El-Seadawy G, Abou-Dina MS, Bishai SS, Ghaleb AF (2006) Implementation of a boundary integral method for the solution of a plane problem of elasticity with mixed geometry of the boundary. *Proc Math Phys Soc Egypt* 85:57–73

60. Helsing J, Ojala R (2008) Corner singularities for elliptic problems: Integral equations, graded meshes, quadrature, and compressed inverse preconditioning. *J Comput Phys* 227(20):8820–8840
61. Helsing J (2011) A fast and stable solver for singular integral equations on piecewise smooth curves. *SIAM J Sci Comput* 33(1): 153–174
62. Li Z-C, Chu P-C, Young L-J, Lee M-G (2010) Combined Trefftz methods of particular and fundamental solutions for corner and crack singularity of linear elastostatics. *Eng Anal Bound Elem* 34:632–654
63. Lee M-G, Young L-J, Li Z-C, Chu P-C (2011) Mixed types of boundary conditions at corners of linear elastostatics and their numerical solutions. *Eng Anal Bound Elem* 35:1265–1278
64. Gillman A, Hao S, Martinsson PG (2014) A simplified technique for the efficient and highly accurate discretization of boundary integral equations in 2D on domains with corners. *J Comput Phys* 256:214–219
65. Bowles JE (1988) *Foundation analysis and design*, 4th edn. McGraw-Hill, New York
66. Kolodziej JA, Kleiber M (1989) Boundary collocation method vs FEM for some harmonic 2-d problems. *Comput Struct* 33(1): 155–168
67. Abou-Dina MS, Ghaleb AF (1999) On the boundary integral formulation of the plane theory of elasticity with applications (analytical aspects). *J Comput Appl Math* 106:55–70
68. Abou-Dina MS, Ghaleb AF (2003) On the boundary integral formulation of the plane theory of elasticity with applications (computational aspects). *J Comput Appl Math* 159:285–317
69. Janke E, Emde F, Lösch F (1968) *Tables of higher functions* edn. L.I, Sedov, Nauka, Moscow. McGraw-Hill, Moscow (in Russian)